Journal of Physical Sciences, Vol. 14, 2010, 145-163
ISSN: 0972-8791, www.vidyasagar.ac.in/journal
Published on December 24, 2010

Flow through a Rotating Curved Square Duct: The Case of Positive Rotation

R. N. Mondal, M. R. Islam, M. S. Uddin and A. K. Datta

Mathematics Discipline; Science, Engineering and Technology School,
Khulna University, Khulna-9208, Bangladesh
Email: rnmondal71@yahoo.com

Received September 27, 2010; accepted November 10, 2010

ABSTRACT

In this paper, a comprehensive numerical study is presented for the flow characteristics through a rotating curved duct with square cross section. Numerical calculations are carried out by using a spectral method and covering a wide range of the Taylor number $0 \le Tr \le 3000$ for two cases of the Dean numbers, *Case I*: $Dn = 1000$ and *Case II*: $Dn = 2000$. A temperature difference is applied across the vertical sidewalls for the Grashof number $Gr = 500$, where the outer wall is heated and the inner one cooled. In this paper, the positive rotation of the duct about the center of curvature is imposed, and the effects of rotation (*Coriolis force*) on the flow characteristics are investigated. As a result, multiple branches of asymmetric steady solutions with two-, three- and four-vortex solutions are obtained. Time evolution calculations as well as phase spaces of the unsteady solutions are obtained, and it is found that in the unstable region the flow undergoes in the scenario "*periodic* $\rightarrow$ *chaotic* $\rightarrow$ *multi-periodic* $\rightarrow$ *periodic* $\rightarrow$ *steady-stable"*, if *Tr* is increased.

Keywords: Rotating curved duct, Dean number, Taylor number, Secondary flow, Time evolution.

1. Introduction

The study of flows and heat transfer through curved ducts and channels is of fundamental interest because of its practical application in chemical, mechanical and biological engineering. Due to engineering application and their intricacy, the flow in a rotating curved duct has become one of the most challenging research fields of fluid mechanics. A quantitative analogy between flows in stationary curved pipes and orthogonally rotating straight pipes has been reported by Ishigaki [1, 2]. Taking this analogy as a basis, this study describes the characteristics of more general and complicated flow in rotating curved ducts, which are relevant to systems involving

helically or spirally coiled pipes rotating about the coil axis. Such rotating flow passages are used in cooling systems in rotating machinery such as gas turbines, electric generators and electric motors. The flow systems are also encountered in separation processes; scientists have paid considerable attention in order to study the characteristics of the flows in these rotating systems. The readers are referred to Berger *et al.* [3] and Nandakumar and Masliyah [4] for some outstanding reviews on rotating and non-rotating curved duct flows.

One of the interesting phenomena of the flow through a curved duct is the bifurcation of the flow because generally there exist many steady solutions due to channel curvature. Many researches have performed experimental and numerical investigation on developing and fully developed curved duct flows. An early complete bifurcation study of two-dimensional (2-D) flow through a curved duct with square cross section was performed by Winters [5]. However an extensive treatment of the flow through a curved square duct was performed by Mondal [6]. He found a close relationship between the unsteady solutions and the bifurcation diagram of steady solutions. Ishigaki [2] examined the flow structure and friction factor numerically for both the counter-rotating and co-rotating curved circular pipe with a small curvature. Selmi *et al.* [7] examined the combined effects of system rotation and curvature on the bifurcation structure of two-dimensional flows in a rotating curved duct with square cross section. Wang and Cheng [8], employing finite volume method, examined the flow characteristics and heat transfer in curved square ducts for positive rotation and found reverse secondary flow for the co-rotation cases.

Studies of unsteady flows in curved ducts, initiated by Lyne [9], have attracted much interest not only for engineering applications to heat exchangers and chemical reactors, but also because of its relevance to hemodynamical problems (Pedley, [10]) i.e. relating to blood flow in human arterial systems. A number of theoretical and experimental studies on periodically unsteady flow in curved tubes have been carried out in last few decades. Belaidi *et al*. [11] studied the flow in tightly coiled 90^0 bend with aspect ratios of 0.5 and 0.25 and a curvature ratio of 1.0. They measured stream wise velocities along the line of symmetry at different stream wise positions and observed the flow oscillations near the inner wall of the duct at a frequency of around 25 Hz. The oscillations seemed to be associated with instability of the secondary flow jet. Kelleher *et al.* [12] were the first to observe experimentally the flow oscillation in a curved channel. Their study was focused on steady low Reynolds number flow with the channel of aspect ratio 40 and a mild curvature. They mentioned that for higher flow rates, the time-dependent flows are observed consisting of stream wise periodic traveling waves superimposed on the Dean vortices. These traveling waves have been studied extensively since 1988 and the results have been helpful in explaining the traveling wave phenomena in a curved duct. Ligrani and Niver [13] investigated the oscillations in the geometry used by Kelleher *et al.* [12]. Ligrani and Niver [13] identified several of other oscillating modes as well as unsteady splitting and merging of Dean vortices.

Time dependent analysis of fully developed curved duct flows was first initiated by Yanase and Nishiyama [14] for a rectangular cross section and by Yanase, Goto and Yamamoto [15] for a circular cross section. In both the studies they investigated unsteady solutions for the case where dual solutions exist. However, the time-dependent behavior of the flow in a curved rectangular duct of large aspect ratios was investigated, in detail, by Yanase *et al.* [16] numerically. They performed time-evolution calculations of the unsteady solutions with and without symmetry condition, and observed that periodic oscillations are available with symmetry condition while aperiodic time evolutions without symmetric condition. Wang and Yang [17, 18] performed numerical as well as experimental investigation on fully developed periodic oscillation in a curved square duct. Flow visualization in the range of Dean numbers from 50 to 500 was carried out in their experiment. They showed, both experimentally and numerically, that the temporal oscillation takes place between symmetric/asymmetric 2-cell and 4-cell flows where there are no stable steady flows. In order to study the time-dependent behavior of the unsteady solutions, recently, Mondal *et al*. [19] performed numerical prediction of the unsteady solutions through a stationary curved square duct flow for the isothermal flows. They showed that periodic solutions turn into chaotic solution through a multi-periodic solution, if the Dean number is increased no matter what the curvature is. They also showed that the chaotic solution becomes weak for small Dean number, while the chaotic solution becomes strong for large Dean number. Very recently, Mondal *et al.* [20] performed a comprehensive numerical study of the non-isothermal flows through a rotating curved square duct for small Grashof number $(Gr = 100)$ and obtained interesting results. In the present study, however, we perform numerical study of the non-isothermal flows through a rotating curved square duct flow for large Grashof number $(Gr = 500)$, because it is expected that more completed flow behavior of the unsteady solutions may occur for large Grashof number case. Transient behavior of the unsteady solutions, such as periodic, multi-periodic or chaotic solutions are yet unresolved for the non-isothermal flow in a rotating curved square duct for large Grashof number. The present study is, therefore, an attempt to fill up this gap with the study of the non-linear behavior of the unsteady solutions by time-evolution calculation.

In the present study, a comprehensive numerical study is presented for fully developed bifurcation structure of two-dimensional (2D) viscous incompressible fluid flow through a rotating curved square duct whose outer wall is heated and inner wall is cooled. Flow characteristics are investigated over a wide range of Taylor number $0 \le Tr \le 3000$ for two cases of the Dean numbers $Dn = 1000$ and $Dn = 2000$ for the Grashof number $Gr = 500$. Studying the effects of rotation on the flow characteristics, caused by the buoyancy and Coriolis forces, is an important objective of the present study.

2. Governing equations

Consider a hydrodynamically and thermally fully developed two-dimensional flow of viscous incompressible fluid through a rotating curved square duct with constant curvature. The height and width of the duct cross section are $2h$ and $2l$, respectively. In the present case, $h = l$ because we are considering a square duct. Figure 1 shows the coordinate system with relevant notations, where C is the center of the duct cross-section and L is the radius of curvature of the duct. The x' and y' axes are taken to be in the horizontal and vertical directions respectively, and z' is the coordinate along the center-line of the duct, i.e., the axial direction. The system rotates at a constant angular velocity Ω_T around the y' axis. It is assumed that the outer wall of the duct is heated while the inner one is cooled. The temperature of the outer wall is $T_0 + \Delta T$ and that of the inner wall is $T_0 - \Delta T$, where $\Delta T > 0$. It is also assumed that the flow is uniform in the axial direction, and that it is driven by a constant pressure gradient $G\left(G = \dfrac{-\partial P'}{\partial z'}\right)$ along the centre-line of the duct.

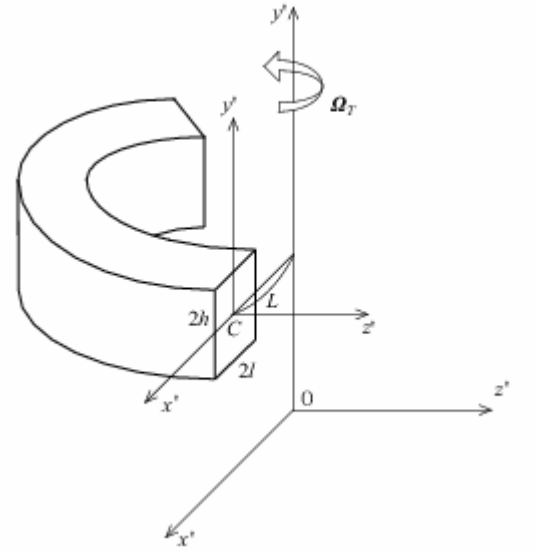

Figure 1. Coordinate system of the rotating curved duct

The dimensional variables are non-dimensionalized by using the representative length l and the representative velocity $U_0 = \dfrac{\upsilon}{l}$, where υ is the kinematics viscosity of the fluid. We introduce the non-dimensional variables defined as:

$$u=\frac{u'}{U_0},\quad v=\frac{v'}{U_0},\quad w=\frac{\sqrt{2\delta}}{\mathrm{U_o}}w',\ x=\left(\frac{x'}{l}-\frac{1}{\delta}\right),\ \bar{y}=\frac{y'}{l},\ z=\frac{z'}{l}$$

$$T=\frac{T'}{\Delta T'},\ t=\frac{U_0}{d}t',\ \delta=\frac{d}{L},\ P=\frac{P'}{\rho {U_0}^2}$$

where u, v and w are the non-dimensional velocity components in the x, y and z directions, respectively; t is the non-dimensional time, P is the non-dimensional pressure, δ is the non-dimensional curvature defined as $\delta=\frac{l}{L}$, and temperature is nondimensionalized by ΔT. Henceforth, all the variables are nondimensionalized if not specified. Since the flow field is uniform in the z direction, the sectional stream function ψ is introduced as

$$u=\frac{1}{1+\delta x}\frac{\partial\psi}{\partial\bar{y}},\quad v=-\frac{1}{1+\delta x}\frac{\partial\psi}{\partial x} \tag{1}$$

Then, the basic equations for the axial velocity w, the stream function ψ and temperature T are expressed in terms of non-dimensional variables as

$$\begin{aligned}(1+\delta x)\frac{\partial w}{\partial t}+\frac{\partial(w,\psi)}{\partial(x,y)}-Dn+\frac{\delta^2 w}{1+\delta x}&=(1+\delta x)\Delta_2 w-\frac{\delta}{1+\delta x}\frac{\partial\psi}{\partial y}w\\&\quad+\delta\frac{\partial w}{\partial x}-\delta Tr\frac{\partial\psi}{\partial y}\end{aligned} \tag{2}$$

$$\begin{aligned}&\left(\Delta_2-\frac{\delta}{1+\delta x}\frac{\partial}{\partial x}\right)\frac{\partial\psi}{\partial t}=-\frac{1}{(1+\delta x)}\frac{\partial(\Delta_2\psi,\psi)}{\partial(x,y)}+\\&+\frac{\delta}{(1+\delta x)^2}\left[\frac{\partial\psi}{\partial y}\left(2\Delta_2\psi-\frac{3\delta}{1+\delta x}\frac{\partial\psi}{\partial x}+\frac{\partial^2\psi}{\partial x^2}\right)-\frac{\partial\psi}{\partial x}\frac{\partial^2\psi}{\partial x\partial y}\right]\\&+\frac{\delta}{(1+\delta x)^2}\times\left[3\delta\frac{\partial^2\psi}{\partial x^2}-\frac{3\delta^2}{1+\delta x}\frac{\partial\psi}{\partial x}\right]-\frac{2\delta}{1+\delta x}\frac{\partial}{\partial x}\Delta_2\psi\\&+w\frac{\partial w}{\partial y}+{\Delta_2}^2\psi-G_r(1+\delta x)\frac{\partial T}{\partial x}+\frac{1}{2}Tr\frac{\partial w}{\partial y},\end{aligned} \tag{3}$$

$$\frac{\partial T}{\partial t}+\frac{1}{(1+\delta x)}\frac{\partial(T,\psi)}{\partial(x,y)}=\frac{1}{\Pr}\left(\Delta_2 T+\frac{\delta}{1+\delta x}\frac{\partial T}{\partial x}\right) \tag{4}$$

where,

$$\Delta_2\equiv\frac{\partial^2}{\partial x^2}+\frac{\partial^2}{\partial y^2},\ \frac{\partial(f,g)}{\partial(x,y)}\equiv\frac{\partial f}{\partial x}\frac{\partial g}{\partial y}-\frac{\partial f}{\partial y}\frac{\partial g}{\partial x} \tag{5}$$

The non-dimensional parameters Dn, the Dean number; Gr, the Grashof number; Tr, the Taylor number and $\Pr$, the Prandtl number, which appear in equations (2) - (4) are defined as:

$$Dn=\frac{Gl^3}{\mu\upsilon}\sqrt{\frac{2l}{L}},\ Gr=\frac{\beta g\Delta T\,l^3}{\upsilon^2},\ \ Tr=\frac{2\sqrt{2\delta}\,\Omega_T l^3}{\upsilon\delta},\ \Pr=\frac{\upsilon}{\kappa} \tag{6}$$

where μ,β,κ and g are the viscosity, the coefficient of thermal expansion, the co-efficient of thermal diffusivity and the gravitational acceleration respectively. μ is the viscosity of the fluid. In the present study, only Dn and Tr are varied, while δ, Gr and $\Pr$ are fixed as $\delta=0.1$, $Gr=500$ and $\Pr=7.0$ (water).

The rigid boundary conditions for w and ψ are used as

$$\begin{aligned}&w(\pm1,y)=w(x,\pm1)=\psi(\pm1,y)=\psi(x,\pm1)\\&=\frac{\partial\psi}{\partial x}(\pm1,y)=\frac{\partial\psi}{\partial y}(x,\pm1)=0\end{aligned} \tag{7}$$

and the temperature T is assumed to be constant on the walls as

$$T(1,y)=1,\ \ T(-1,y)=-1,T(x,\pm1)=x \tag{8}$$

It should be noted that Eqs. (2), (3) and (4) are invariant under the transformation of the variables

$$\left.\begin{aligned}y&\Rightarrow -y\\w(x,y,t)&\Rightarrow w(x,-y,t),\\\psi(x,y,t)&\Rightarrow -\psi(x,-y,t),\\T(x,y,t)&\Rightarrow -T(x,-y,t)\end{aligned}\right\} \tag{9}$$

Therefore, the case of heating the inner sidewall and cooling the outer sidewall can be deduced directly from the results obtained in this study. Equations (2) - (4) would

serve as the basic governing equations which are solved numerically as discussed in the following section.

3. Numerical Calculations

In order to solve the Eqs. (2) - (4) numerically, the spectral method is used. This is the method which is thought to be the best numerical method for solving the Navier-Stokes as well as energy equations (Gottlieb and Orszag [21]). By this method the variables are expanded in a series of functions consisting of Chebyshev polynomials. That is, the expansion functions $\phi_n(x)$ and $\psi_n(x)$ are expressed as

$$\left.\begin{aligned}\phi_n(x) &= (1-x^2)\,C_n(x),\\ \psi_n(x) &= (1-x^2)^2 C_n(x)\end{aligned}\right\} \tag{10}$$

where $C_n(x) = \cos(n\cos^{-1}(x))$ is the n^{th} order Chebyshev polynomial. $w(x,y,t)$, $\psi(x,y,t)$ and $T(x,y,t)$ are expanded in terms of the expansion functions $\phi_n(x)$ and $\psi_n(x)$ as:

$$\left.\begin{aligned}w(x,y,t) &= \sum_{m=0}^{M}\sum_{n=0}^{N} w_{mn}(t)\,\varphi_m(x)\,\varphi_n(y)\\ \psi(x,y,t) &= \sum_{m=0}^{M}\sum_{n=0}^{N} \psi_{mn}(t)\,\psi_m(x)\,\psi_n(y).\\ T(x,,y,t) &= \sum_{m=0}^{M}\sum_{n=0}^{N} T_{mn}\,\varphi_m(x)\,\varphi_n(y)+x\end{aligned}\right\} \tag{11}$$

where M and N are the truncation numbers in the x and y directions respectively, and w_{mn}, ψ_{mn} and T_{mn} are the coefficients of expansion. In order to obtain a steady solution $\overline{w}(x,y), \overline{\psi}(x,y)$ and $\overline{T}(x,y)$, the expansion series (11) is submitted into the basic Eqs. (2), (3) and (4), and the collocation method (Gottlieb and Orszag [21]) is applied. As a result, a set of nonlinear algebraic equations for w_{mn}, ψ_{mn} and T_{mn} are obtained. The collocation points (x_i, y_j) are taken to be

$$\left.\begin{aligned}x_i &= \cos\left[\pi\left(1-\frac{i}{M+2}\right)\right], \qquad i = 1,\ldots,M+1\\ y_j &= \cos\left[\pi\left(1-\frac{j}{N+2}\right)\right], \qquad j = 1,\ldots,N+1\end{aligned}\right\} \tag{12}$$

where $i = 1, \ldots, M+1$ and $j = 1, \ldots, N+1$. Steady solutions are obtained by the Newton-Rapshon iteration method assuming that all the variables are time independent. The convergence is assured by taking $\varepsilon_p < 10^{-10}$, where subscript p denotes the iteration number and ε_p is defined as:

$$\varepsilon_p = \sum_{m=0}^{M}\sum_{n=0}^{N}\left[\left(w_{mn}^{(p+1)} - w_{mn}^{p}\right)^2 + \left(\psi_{mn}^{(p+1)} - \psi_{mn}^{p}\right)^2 + \left(T_{mn}^{(p+1)} - T_{mn}^{p}\right)^2\right] \tag{13}$$

In the present numerical calculation, for sufficiently accuracy of the solutions, we take $M = 20$ and $N = 20$. Finally, in order to calculate the unsteady solutions, The Crank-Nicolson and Adams-Bashforth methods together with function expansion (11) and the collocation methods are applied to Eqs. (2) to (4).

4. Flux through the Duct

The dimensional total flux Q' through the duct in the rotating coordinate system is calculated by:

$$Q' = \int_{-d}^{d}\int_{-d}^{d} w'\,dx'\,dy' = v\,dQ \tag{14}$$

where,
$$Q = \int_{-1}^{1}\int_{-1}^{1} w\,dx\,dy \tag{15}$$

is the dimensionless total flux. The mean axial velocity $\overline{w}'$ is expressed as

$$\overline{w}' = \frac{Qv}{4d} \tag{16}$$

In the present study, Q is used to denote the steady solution branches and to pursue the time evolution of the unsteady solutions.

5. Results and Discussion

We take a curved duct of square cross section and rotate it around the center of curvature with an angular velocity Ω_T. In the present study, we investigate the flow characteristics for the case of positive rotation of the duct (positive Tr), and discuss the numerical prediction of flow phenomena for two cases of the Dean numbers, *Case I*: $Dn = 1000$ and *Case II*: $Dn = 2000$, over a wide range of the Taylor

number $0 \le Tr \le 3000$. Thus, an interesting and complicated flow behavior will be expected if the duct rotation is considered for these cases.

5.1 Case *I*: $Dn = 1000$

5.1.1 Steady solutions

By using the path continuation technique as discussed by Keller [22], we obtain two branches of steady solutions for $Dn = 1000$ over the Taylor number $0 \le Tr \le 3000$. The two steady solution branches are named the *first steady solution branch* (first branch, thin solid line) and the *second steady solution branch* (second branch, dashed line), respectively. It should be noted here that Mondal *et al*. [23] obtained two branches of steady solutions for the non-isothermal flow through a curved square duct without rotation. Figure 2 shows the flux Q through the duct versus the Taylor number Tr for $Dn = 1000$. It is found that the first branch consists of asymmetric two-vortex solutions while the second branch is composed of asymmetric two-, three-, and four- vortex solutions. These vortices are generated due to the combined action of the *centrifugal force* and *Coriolis force*.

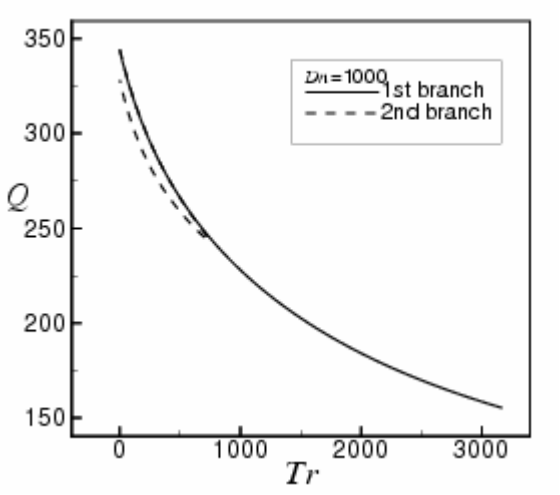

Figure 2: Steady solution branches for $Dn = 1000$ and $Gr = 500$.

5.1.2 Unsteady solutions by Time evolution calculation

In order to study the non-linear behavior of the unsteady solutions, time-evolution calculations are performed for Tr in the range $0 \le Tr \le 3000$ at $Dn = 1000$. The first steady solution branch is partly unstable at the small value of Tr ($Tr \le 15.3$). Thus in the unstable region, we perform time evolution of Q for $Tr = 0$, which is shown in Fig. 3(a). It is found that the flow is time periodic. In order to view the multi-periodic oscillation more clearly, an enlargement of Fig. 3(a)

is shown in Fig. 3(b). In Fig. 3(a), the relationship between the periodic solution and the steady states, that is the values of Q for the steady solutions at $Tr = 0$, are also shown by straight lines using the same kind of lines as were used in the bifurcation diagram in Fig. 2. As seen in Fig. 3(a), the multi-periodic solution at $Tr = 0$ oscillates in the region between the upper and the lower parts of the second steady solution branch, and the upper part of the second branch or the first branch plays a role of an envelop of this periodic oscillation.

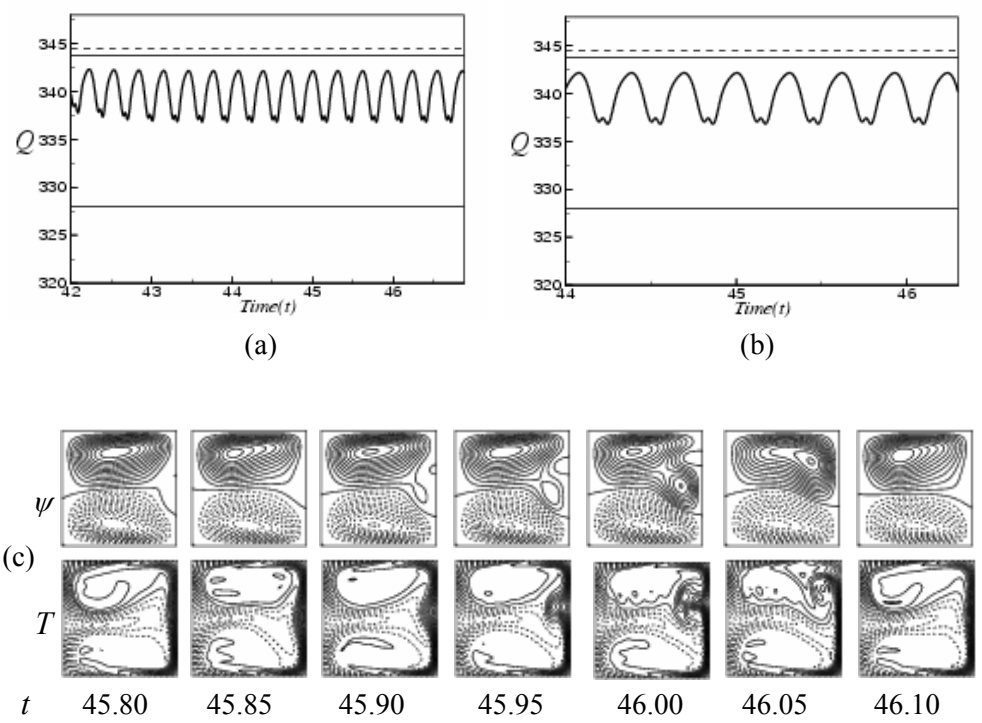

Figure 3: Unsteady solution for $Dn = 1000$ and $Tr = 0$. (a) Time evolution of Q and the values of Q for the steady solutions. (b) An enlargement of Fig. 3(a). (c) Contours of secondary flow (top) and temperature profile (bottom) for one period of oscillation at $45.80 \le t \le 46.10$.

Then, in order to see the change of the flow characteristics as, time proceeds, contours of typical secondary flow and temperature distribution are shown in Fig. 3(c) for one period of oscillation at $Tr = 0$, where it is seen that the periodic solution at $Tr = 0$ oscillates between asymmetric two- and four-vortex solutions. It should be noted here that the result of time evolution for $Dn = 1000$, obtained in

the present study for $Gr = 500$ and $Tr = 0$, has a similarity with that of the result obtained by Mondal *et al*. [20] for $Gr = 100$ and $Tr = 100$.

In order to be sure whether the flow oscillation presented in Fig. 3 for $Dn = 1000$ is periodic or multi-periodic, we now discuss the transitional behavior of the unsteady solutions by drawing phase spaces. In Fig. 4, the oscillation for $Dn = 1000$ shown in Fig. 3, is explicitly exhibited by drawing the orbit of the solution in the phase spaces, where the abscissa is Q and the ordinate is γ. The orbits are drawn by tracing the time evolution of a solution. As seen in Fig. 4, the flow is clearly multi-periodic.

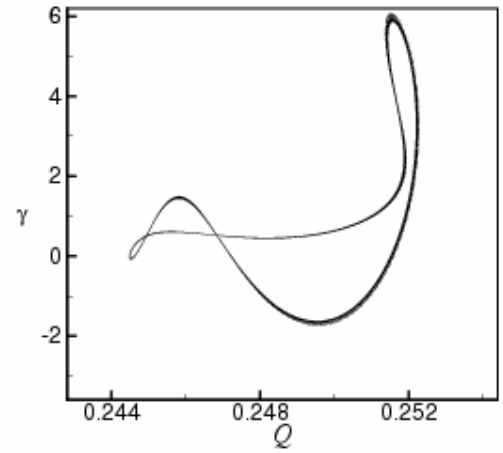

Figure 4: Phase plots in the $Q - \gamma$ plane for $Dn = 2000$ and Tr =0, where $\gamma = \iint \psi \, dx \, dy$.

5.2 Case *I*: $Dn = 2000$

5.2.1 Steady solutions

We obtain four branches of steady solutions for $Dn = 2000$ and $Gr = 500$ over a wide range of Tr for $0 \le Tr \le 3000$. The bifurcation diagram of steady solutions is shown in Fig. 5. The four steady solution branches are named the *first steady solution branch* (first branch, thick solid line), the *second steady solution branch* (second branch, dashed line), the *third steady solution branch* (third branch, thin solid line) and the *fourth steady solution branch* (fourth branch, dash dotted line), respectively.

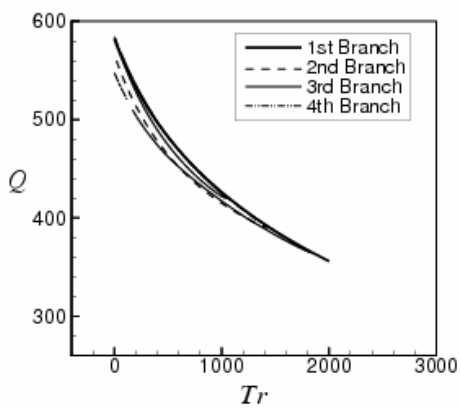

Figure 5: Steady solution branches for $Dn = 2000$ and $Gr = 500$.

The solution branches are distinguished by the nature and number of secondary flow vortices appearing in the cross section of the duct. In this regard, it should be noted that Mondal *et al.* [20] also obtained four braches of steady solutions for $Gr = 100$, but our result is different from theirs in the formation of solution structure and secondary vortices. This is due to the cause of strong buoyancy force i.e. we consider large Grashof number. It is found that there exist two- and four-vortex solutions on various branches. The first branch consists of asymmetric two-vortex solutions. The second branch is composed of asymmetric two-, three- and four-vortex solutions. The third branch is composed of asymmetric two- and four-vortex solutions and the forth branch is composed of asymmetric four-vortex solutions.

5.2.2 Unsteady solutions by Time evolution calculation

In order to investigate the non-linear behavior of the unsteady solutions, we perform time-evolution calculations of the unsteady solutions for $Dn = 2000$ at $0 \le Tr \le 3000$. Time evolution of Q for $Dn = 2000$ and $Tr \le 279$ shows that the value of Q quickly approaches steady-state no matter what the initial condition we use.

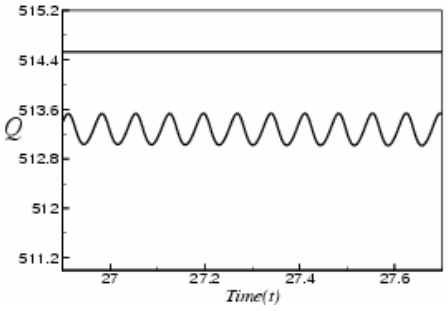

(a)

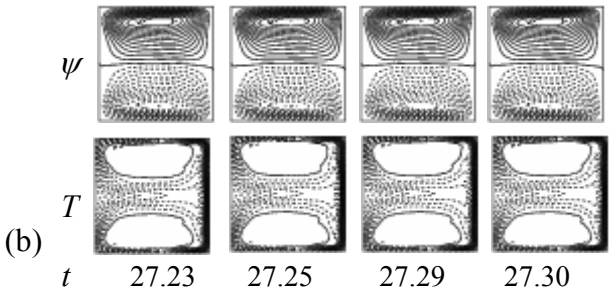

Figure 6: Unsteady solution for $Dn = 1000$ and $Tr = 300$ (a) Time evolution of Q and the values of Q for steady solutions. (b) Contours of secondary flow (top) and temperature profile (bottom) for one period of oscillation at $27.23 \le t \le 27.30$.

Then, in order to see what happens when all the steady solutions are linearly unstable in the region $279 \le Tr \le 922.80$, time evolutions of Q are then performed for $Tr = 300, 500, 700$ and 900. Figure 6(a) shows the time-evolution of Q for $Tr = 300$, where it is seen that the flow oscillates periodically. In the same figure, to observe the relationship between the periodic solution and the steady states, the values of Q for the steady solution branch at $Tr = 300$ are shown by straight lines using the same kind of lines as were used in the bifurcation diagram in Fig. 4. As seen in Fig. 6(a), the unsteady solution at $Tr = 300$ oscillates in the region below the upper part and above the lower part of the third steady solution branch. To observe the periodic change of the flow characteristics and temperature distributions, contours of typical secondary flow and temperature profile for one period of oscillation at $27.23 \le t \le 27.30$ are shown in Fig. 6(b), where it is seen that the periodic oscillation at $Tr = 300$ is an asymmetric two-vortex solution.

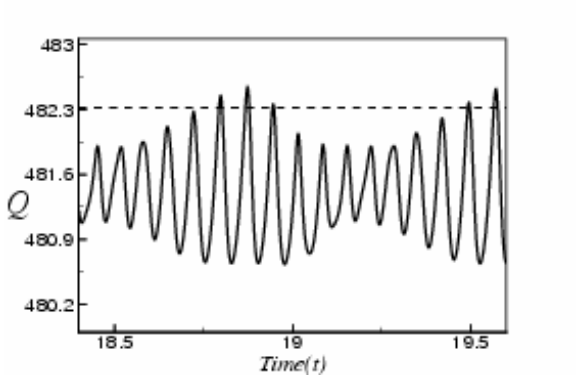

(a)

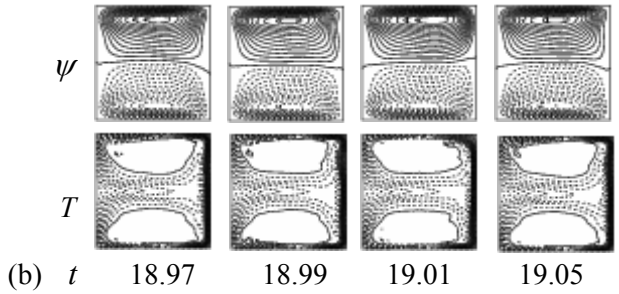

Figure 7: Unsteady solution for $Dn = 1000$ and $Tr = 500$ (a) Time evolution of Q and the values of Q for steady solutions. (b) Contours of secondary flow (top) and temperature profile (bottom) for one period of oscillation at time $18.97 \le t \le 19.05$.

Next, the time evolution of Q, together with the values of Q for the steady solutions indicated by straight lines, are shown in Fig. 7(a) for $Tr = 500$. It is found that the flow oscillates periodically. The associated secondary flow patterns and temperature profiles at $18.97 \le Tr \le 19.05$ are shown in Fig. 7(b). It is found that the unsteady flow at $Tr = 500$ also oscillates between the asymmetric two-vortex solutions. Time evolution of Q, together with the values of Q for the steady solution branches indicated by straight lines, are shown in Fig. 8(a) for $Tr = 700$. It is found that the flow oscillates multi-periodically in the region along the values of Q on the upper parts of the first steady solution branch. The associated secondary flow patterns and temperature profiles at $10.55 \le t \le 10.63$ are shown in Fig. 8(b). It is found that the unsteady flow at $Tr = 700$ also oscillates between the asymmetric two-vortex solutions.

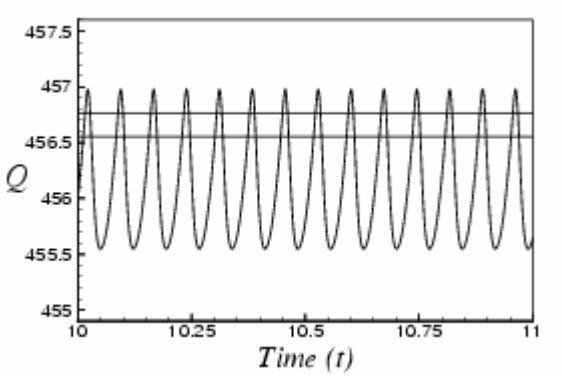

(a)

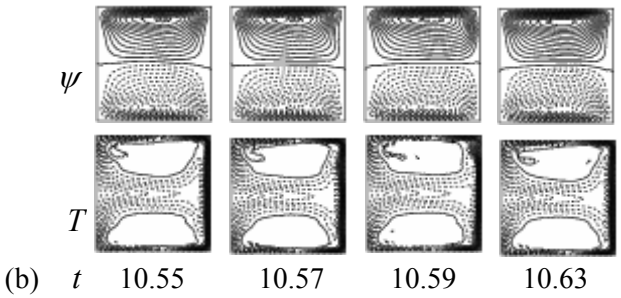

Figure 8: Unsteady solution for $Dn = 1000$ and $Tr = 700$ (a) Time evolution of Q and the values of Q for the steady solutions. (b) Contours of secondary flow (top) and temperature profile (bottom) for one period of oscillation at time $10.55 \le t \le 10.63$.

Similarly, time evolution of Q, together with the values of Q for the steady solution branches indicated by straight lines, are shown in Fig. 9(a) for $Tr = 900$. It is found that the flow oscillates multi-periodically in the region along the values of Q on the lower part of the forth steady solution branch. The associated secondary flow patterns and temperature profiles for one period at $7.81 \le t \le 7.89$ are shown in Fig. 9(b). It is found that the unsteady flow at $Tr = 900$ also oscillates between the asymmetric two-vortex solutions. Time evolutions of Q are then performed at several values Tr for $922.90 \le Tr \le 3000$, and it is found that the value of Q approaches steady state. The reason is that the steady flow is linearly stable on the first steady solution branch in this region.

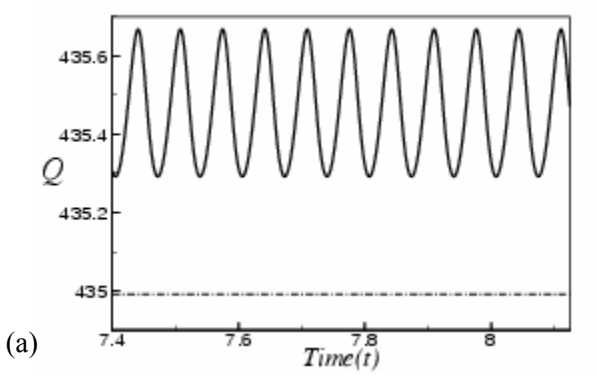

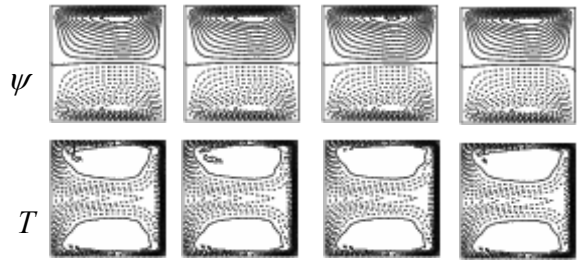

Figure 9: Unsteady solution for $Dn = 1000$ and $Tr = 900$ (a) Time evolution of Q and the values of Q for the steady solutions. (b) Contours of secondary flow (top) and temperature profile (bottom) for one period of oscillation at $7.81 \le t \le 7.89$.

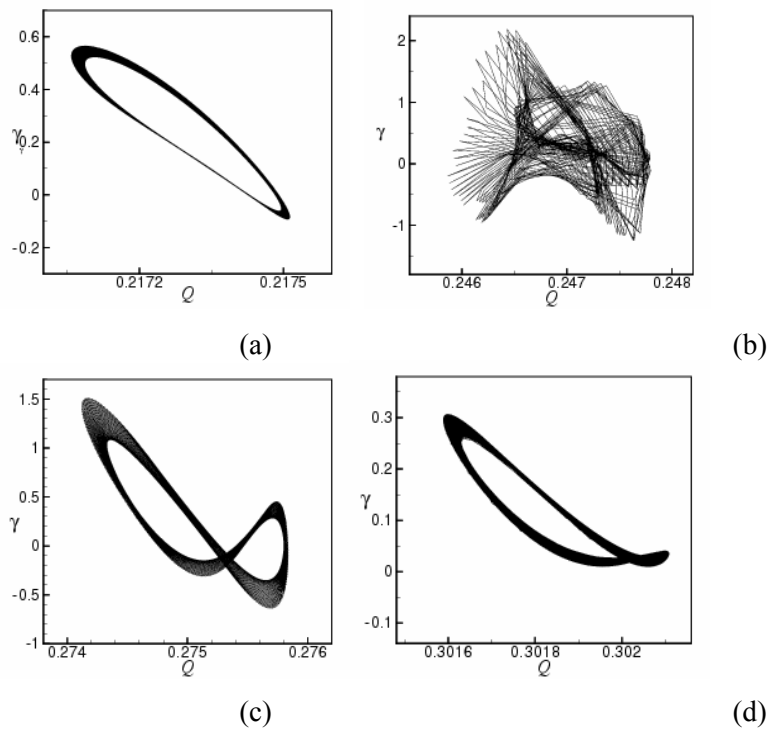

Figure 10: Phase plots in the $Q - \gamma$ plane for $Dn = 2000$, where $\gamma = \iint \psi \, dx \, dy$
(a) $Tr = 300$, (b) $Tr = 500$, (c) $Tr = 700$, (d) $Tr = 900$.

We now discuss the unsteady flow behavior by drawing phase spaces for $Dn = 2000$. The change of the flow state from periodic oscillation to transitional chaos and then multi-periodic or periodic oscillation is explicitly exhibited by drawing the orbit of the solution in the phase spaces as shown in Figs. 10(a-d) for Tr = 300, 500, 700 and 900. The orbits are drawn by tracing the time evolution of the solutions. As seen in Fig. 10(a), a periodic solution is seen for Tr = 300; for Tr = 500, however, an entangled chaotic orbit overlaps the multi-periodic orbit which is termed as *transitional chaos* (Mondal *et al.* [19]), though the time evolution result presented in Fig. 7 for Tr = 500 seems to be multi-periodic but actually it is chaotic solution as seen from Fig. 10(b). Similarly, the time evolution result presented in Fig. 8 for Tr = 700 seems to be periodic but their phase space (Fig. 10(c)) shows that it is multi-periodic. Time evolution result for Tr = 900 (Fig. 9), on the other hand, shows that it is periodic but actually it is apparently multi-periodic as seen in Fig. 10(d) for Tr = 900.

6. Conclusions

A comprehensive numerical study on the fully developed two-dimensional flow of viscous incompressible fluid through a rotating curved square duct has been performed by using the spectral method, and covering a wide range of the Taylor number, $0 \le Tr \le 3000$ and the Dean number $0 < Dn \le 3000$ for two cases of the Dean numbers, $Dn = 1000$ and $Dn = 2000$. A temperature difference is applied across the vertical sidewalls for the Grashof number $Gr = 500$, where the outer wall is heated and the inner one cooled. First, steady solutions are obtained and then in order to study the nonlinear behavior of the unsteady solutions time evolution calculations are performed.

After a comprehensive survey over the range of the parameters, we obtained two branches of asymmetric steady solutions with two-, three- and four-vortex solutions for the rotating curved square duct flows for $Dn = 1000$ and $Gr = 500$. Then we performed time evolution calculation of the unsteady solutions, and it is found that the unsteady flow becomes multi-periodic oscillation before turning to steady state. Then we investigated flow characteristics for $Dn = 2000$, and we obtained four branches steady solutions with the same number of vortices but different in nature in the formation of secondary vortices at the cross section of the duct. In order to study the non-linear behavior of the unsteady solutions, we then performed time-evolution calculations as well as phase spaces of the solutions in the unstable region, and it is found that unsteady flow turns into steady-stable in the scenario "*periodic* $\rightarrow$ *chaotic* $\rightarrow$ *multi-periodic* $\rightarrow$ *steady-stable"*, if Tr is increased. Drawing the phase spaces was found to be more fruitful for the investigation of unsteady flow behavior. In this regard, it should be noted that irregular oscillation of the flow through a curved duct has been observed experimentally by Ligrani and Niver [13] for the large aspect ratio and by Wang and Yang [18] for the curved square duct flow.

Acknowledgement: The author would like to gratefully acknowledge the financial support from the Bangladesh Ministry of Science and Information & Communication Technology to conduct this research work under the special allocation of 2008-2009 (Code No.: 3-2605-3993-5921) to Rabindra Nath Mondal.

REFERENCES

1. Ishigaki, H. 1983. Fundamental characteristics of laminar flows in a rotating curved pipe. *Trans. JSME,* Vol. 59-561-B, pp. 1494-1501.
2. Ishigaki, H. 1996. Laminar flow in rotating curved pipes. *Journal of Fluid Mechanics,* Vol. 329, pp. 373-388.
3. Berger, S.A., Talbot, L., Yao, L. S. 1983. Flow in Curved Pipes, *Annual. Rev. Fluid. Mech*., Vol. 35, pp. 461-512.
4. Nandakumar, K. and Masliyah, J. H. 1986. Swirling Flow and Heat Transfer in Coiled and Twisted Pipes, *Adv. Transport Process*., Vol. 4, pp. 49-112.
5. Winters, K. H. 1987. A Bifurcation Study of Laminar Flow in a Curved Tube of Rectangular Cross-section, *Journal of Fluid Mechanics*, **Vol.** 180, 343-369.
6. Mondal, R. N. 2006. Isothermal and Non-isothermal Flows Through Curved ducts with Square and Rectangular Cross Sections, *Ph.D. Thesis*, Department of Mechanical Engineering, Okayama University, Japan.
7. Selmi, M. and Namdakumar, K. and Finlay W. H. 1994. A bifurcation study of viscous flow through a rotating curved duct, *J. Fluid Mechanics,* Vol. 262, pp. 353-375.
8. Wang, L. Q. and Cheng, K.C. 1996. Flow Transitions and combined Free and Forced Convective Heat Transfer in Rotating Curved Channels: the Case of Positive Rotation, *Physics of Fluids*, Vol. 8, pp. 1553-1573.
9. Lyne,W.H. 1970. Unsteady viscous flow in a curved pipe, *Journal of Fluid Mechanics*, Vol. 45(1), pp. 13-31.
10. Pedley, T. J. 1980. The Mechanics of Large Blood Vessel, P.235. Cambridge University Press.
11. Belaidi, A., Jahnson, M. W. and Humphrey, J.A.C. 1992. Flow instability in a curved duct of rectangular cross section, *ASME Trans., Journal of Fluids Engineering,* Vol. 114, pp. 585-591.
12. Kelleher, M.D., Flentle, D.L. and McKee, R.J. 1980. An experimental study of the secondary flow in a curved rectangular channel, *Trans.* ASME, *Journal of Fluids Engineering,* Vol. 102, pp. 92-96.
13. Ligrani, P. M. and Niver, R.D. 1988. Flow visualization of Dean vortices in a curved channel with 40 to1 aspect ratio, *Physics of Fluids A*, Vol. 31(12), pp. 3605-3617.
14. Yanase, S. and Nishiyama, K. 1988. On the bifurcation of laminar flows through a curved rectangular tube, *J. Phys. Soc*. *Japan*, Vol. 57(11), pp. 3790-3795.
15. Yanase, S., Goto, N. and Yamamoto, K. 1989. Dual solutions of the flow through a curved tube, *Fluid Dynamics Research*, Vol. 5, pp. 191-201.

16. Yanase, S., Kaga, Y. and Daikai, R. 2002. Laminar flow through a curved rectangular duct over a wide range of the aspect ratio, *Fluid Dynamics Research*, Vol. 31**, pp.** 151-183.
17. Wang, L. and Yang, T. 2004. Bifurcation and stability of forced convection in curved ducts of square cross section, *Int. journal of Heat Mass Transfer*, Vol. 47, pp. 2971-2987.
18. Wang, L. and Yang, T. 2005. Periodic Oscillation in Curved Duct Flows, *Physica D*, Vol. 200, pp. 296-302.
19. Mondal, R. N., Kaga, Y., Hyakutake, T.and Yanase, S. 2007. Bifurcation Diagram for Two- dimensional Steady Flow and Unsteady Solutions in a Curved Square Duct, *Fluid Dynamics Research*. Vol. 39, pp. 413-446.
20. Mondal, R. N., Alam M. M. and Yanase, S. 2007. Numerical prediction of non-isothermal flows through a rotating curved duct with square cross section, *Thommasat Int. J. Sci and Tech.*, Vol. 12(3), pp. 24-43.
21. Gottlieb, D. and Orazag, S. A. 1977. Numerical Analysis of Spectral Methods, *Society for Industrial and Applied Mathematics*, Philadelphia.
22. Keller, H. B. 1987. Lectures on Numerical Methods in Bifurcation Problems, *Springer*, Berlin.
23. Mondal, R. N., Kaga, Y., Hyakutake, T. and Yanase, S. 2006. Effects of curvature and convective heat transfer in curved square duct flows, *Trans. ASME, Journal of Fluids engineering*, Vol. 128(9), pp. 1013-1022.